ISSN: 2414-1895 DOI: 10.6919/ICJE.202504_11(4).0037

Preparation and Characterisation of Gradient Silver-modified ZIF-8 Nanoparticles and Their Antibacterial Properties

Wenjing Bai, Zhongyi Zhao

School of Materials and Chemistry, School of Materials and Chemistry, University of Shanghai for Science and Technology, Shanghai 200093, China

Abstract

Titanium alloys are widely used in medical implants due to their excellent biocompatibility and corrosion resistance. However, their biological inertness makes bonding with natural bone ineffective and susceptible to bacterial infection. In order to improve its performance in implants, this study explores the application of gradient silver-modified ZIF-8 nanoparticles (Ag@ZIF-8 NPs) on the surface of titanium alloys through their preparation and characterisation. ZIF-8 was used as the base material and 1%, 5% and 10% silver-modified ZIF-8 NPs were obtained by doping with different concentrations of silver.It was shown that Ag@ZIF-8 NPs remained stable in the framework structure of ZIF-8, while silver doping significantly enhanced their antibacterial properties. The structures were analyzed in detail by scanning electron microscopy SEM, XRD and FT-IR, and their antimicrobial efficacy against Escherichia coli and Staphylococcus aureus was assessed by plate counting method.The results showed that the increase of silver concentration significantly improved the antimicrobial performance, especially for 10% Ag@ZIF-8 samples. This study provides a new idea for the development of surface-modified materials for titanium alloys, which has important application prospects, especially in the enhancement of antimicrobial properties of medical implants.

Keywords

ZIF-8; Antibacterial; Titanium Alloys.

1. Introduction

Titanium alloys are widely used in fields such as orthopaedic and dental implants due to their excellent mechanical properties, biocompatibility and corrosion resistance [1]. However, as a biologically inert material, titanium alloy surfaces are difficult to integrate effectively with natural bone tissue, limiting its effectiveness in implant applications. More critically, common implant infections can lead to bacterial growth, triggering inflammation at the implant site and ultimately leading to implant failure. Therefore, the development of implant materials with antimicrobial properties has become a key direction to solve the problem of implant infection.

Among many nanocarrier materials, ZIF-8 stands out due to its unique physicochemical properties.ZIF-8 is a porous crystalline material formed by the coordination self-assembly of Zn^{2+} with 2-methylimidazole, which possesses a high specific surface area, homogeneous pore distribution, excellent thermal and chemical stability [2]. Its structure is similar to that of inorganic zeolites and it has a responsive drug release function in a weak acidic environment, which makes it show great potential in the field of drug delivery. In addition, ZIF-8 can be synthesised under mild conditions with good biocompatibility and can be efficiently loaded with a variety of active substances such as chemotherapeutic drugs, acoustic sensitiser molecules and biological enzymes [3].

ISSN: 2414-1895 DOI: 10.6919/ICJE.202504_11(4).0037

Silver nanoparticles (Ag NPs) have been the focus of research in the medical field due to their excellent antimicrobial properties. Ag NPs can efficiently contact with microorganisms and release silver ions, thus enhancing the bactericidal activity [4]. However, with their wide application, studies on the toxicity, cytotoxicity, and environmental effects of Ag NPs remain an urgent issue. Therefore, an in-depth investigation of the mechanism of action of Ag NPs and their potential effects on cells and tissues is essential to ensure their safe application [5].

In this study, gradient silver-modified ZIF-8NPs (Ag@ZIF-8) were prepared by on the surface of titanium alloy. The surface structure, chemical composition and antibacterial properties of Ag@ZIF-8 nanoparticles are characterised and discussed in detail.

2. Materials and Methods

2.1 Sample Preparation

0.1 g of $Zn(NO_3)_2$-$6H_2O$ and 2.3 g of 2-methylimidazole were added into 20 mL of deionised water and stirred for 15 min, and the homogeneous 2-methylimidazole solution was quickly poured into the $Zn(NO_3)_2$-$6H_2O$ solution, and stirred vigorously at room temperature for 2 h. After the mixed solution gradually appeared milky white, it was centrifuged at 9,000 rpm for 15 min, and then dried in an oven at 60°C for 12 h. ZIF-8 powder solid was obtained. The fresh precipitate was washed with deionised water to continue centrifugation and dried in an oven at 60°C for 12 h to obtain ZIF-8 powder solid, which was poured into a mortar and ground to powder particles for spare use. Weigh 0.011g CH_3COOAg, add 2mL of deionised water to dissolve, add 10mL of ethanol to it and continue stirring for 5min.0.1 g of ZIF-8 was dispersed in 10 mL of dimethyl sulfoxide, which was added to the prepared ethanol-water solution of CH_3COOAg with vigorous stirring at room temperature for 2 h. The Ag was reduced by simulated sunlight irradiation under a 300 W xenon lamp light source for 60 min. Finally, it was centrifuged at 9000 rpm for 15 min, and the unreacted solution was washed with deionised water and then continued to be centrifuged and dried in an oven at 50 °C for 12 h to obtain the Ag@ZIF-8 solid powder, which was poured into a mortar and grinded to powder particles for spare use. The added CH_3COOAg accounted for 10% of the mass of the total precursor, and the product was labelled as 10% Ag@ZIF-8. Using the same method, 1% Ag@ZIF-8 and 5% Ag@ZIF-8 could be prepared, i.e., 0.0053 g and 0.025 g of CH_3COOAg were added, respectively.

2.2 Surface Morphology and Compositional Structure Analysis

The surface morphology of the coatings was observed by scanning electron microscopy (SEM), and the elemental distribution was analysed by energy spectroscopy (EDS) coupled with SEM. Phase analysis was performed by X-ray diffraction (XRD). The molecular structure of the coatings was analyzed by Fourier Transform Infrared Spectroscopy (FTIR).

2.3 Evaluation of Antimicrobial Properties

Escherichia coli (E. coli) and Staphylococcus aureus (S. aureus) were selected as representative Gram-negative and Gram-positive bacteria to assess the antibacterial properties of the samples. The test samples were placed in 24-well plates with 2 mL of bacterial suspension. The well plates were then incubated at 37°C for 24 hours. At the end of incubation, the samples were rinsed with sterile PBS. The rinse solution was collected into a centrifuge tube, vortexed and mixed for dilution. 30 μL of the diluted solution was spread on LB agar plates and the plates were inverted and incubated at 37°C. Bacterial growth and colony formation was assessed by visual observation and colony counting at the end. The antimicrobial activity of the samples was assessed by plate counting method and the antimicrobial rate (R) was calculated by the following formula:

$$R\% = \frac{D - D_W}{D} \times 100\% \quad (1)$$

where D and Dw denote the number of viable bacterial colonies on the control and test samples, respectively.

3. Physical Structure Analysis

3.1 Section Headings

The figure1 shows the XRD patterns of ZIF-8 and silver-modified ZIF-8 samples (Ag@ZIF-8) with different concentrations. The pure ZIF-8 exhibits distinct diffraction peaks at 7.38°, 10.35°, 12.71°, 14.61°, 16.39°, 18.05°, 22.14°, 24.42°, and 26.70°, which correspond to the (011), (002), (112), (022), (013), (222), (114), (233), and (134) crystal planes of ZIF-8, respectively [6]. These peaks match the standard XRD pattern of ZIF-8, indicating that ZIF-8 has a stable crystal structure. For the XRD patterns of ZIF-8 modified with different concentrations of silver, the positions of the major diffraction peaks changed less, indicating that the introduction of silver did not significantly change the overall crystal structure of ZIF-8.Ag^+ replaced a small amount of Zn^{2+} in the framework of ZIF-8 by means of ion-exchange or by loading on the surface of ZIF-8 and in the pores. The similar ionic radii of Ag^+ and Zn^{2+} result in a possible slight broadening of the diffraction peaks in the XRD patterns. However, at the same time, the low silver loading does not allow the characteristic peaks of silver to be clearly shown in the pattern.

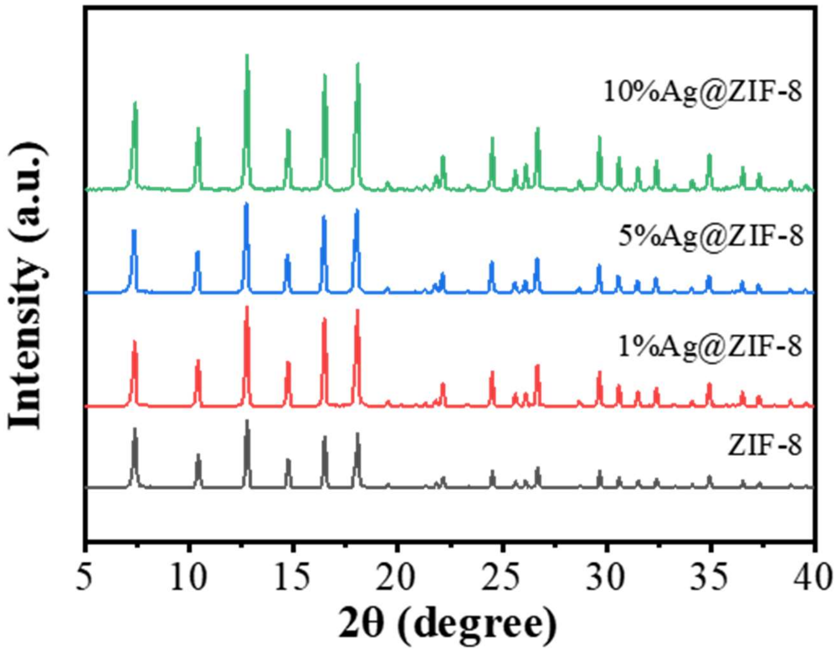

Figure 1. XRD patterns of Ag@ZIF-8 NPs with different silver concentrations

The Fourier transform infrared (FT-IR) absorption spectra of ZIF-8 and silver-modified ZIF-8 (Ag@ZIF-8) samples with different concentrations of silver in the wavelength range of 4000 to 450 cm^{-1} are presented in the figure 2. Firstly, the FT-IR spectra of ZIF-8 showed absorption peaks at 763 cm^{-1} and 1146 cm^{-1}, respectively, attributed to the stretching vibration of the C-N bond in the imidazole ring, while the absorption peak at 1580 cm^{-1} corresponded to the stretching vibration of the C=N bond. In addition, the absorption band of ZIF-8 at 2929 cm^{-1} can be attributed to the aromatic C-H stretching vibration in the imidazole ring [7]. All the characteristic FT-IR peaks of ZIF-8 are in agreement with the results reported in the literature. In the Ag@ZIF-8 sample, the Ag-N vibrational peak is weaker due to the weak coordination force between Ag^+ and 2-methylimidazole ligand, which may fail to be clearly visible in the spectra.

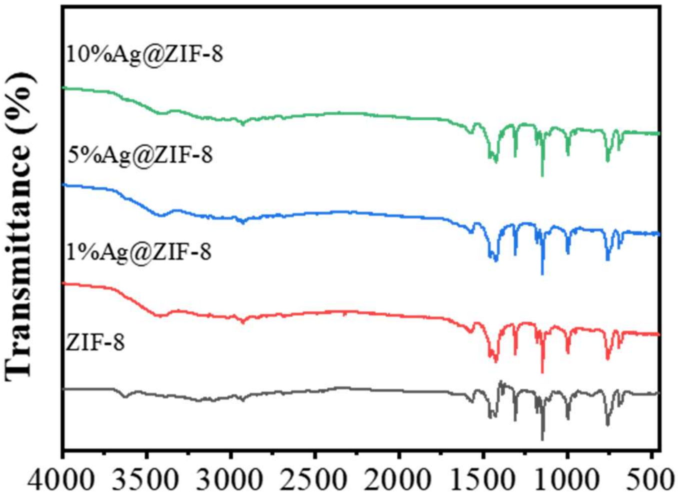

Figure 2. FT-IR patterns of Ag@ZIF-8 NPs with different silver concentrations

3.2 Morphology Analysis

The figure 3 demonstrates the SEM images of ZIF-8 and different concentrations of silver-modified ZIF-8 (Ag@ZIF-8) nanoparticles. The results show that the ZIF-8 nanoparticles have a regular orthododecahedral shape with an average particle size of about 0.7-1.2 μm and a smooth and uniform surface. Compared with pure ZIF-8, during the introduction of Ag^+, Ag^+ was reduced to Ag NPs and loaded on the surface or in the pores of ZIF-8, resulting in minor distortions of the local lattice and particle adsorption. This phenomenon was more pronounced with increasing Ag concentration, but the overall ZIF-8 crystal structure remained relatively stable. Further analysis showed that Ag^+ had a weaker binding affinity for the 2-methylimidazole ligand than Zn^{2+} and a slower deprotonation process, resulting in the introduction of Ag^+ significantly decreasing the crystal nucleation rate of ZIF-8, which in turn delayed the crystal growth and increased the inhomogeneity. This suggests that Ag modification has an inhibitory effect on the crystal growth of ZIF-8.

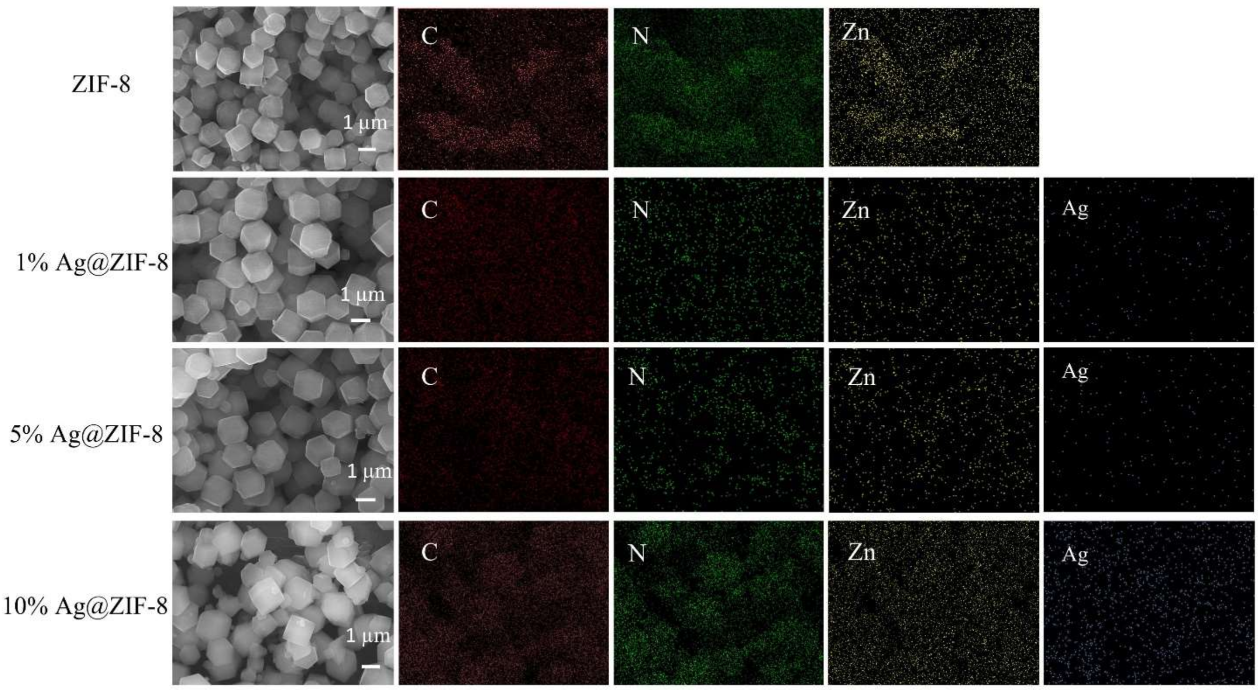

Figure 3. SEM of Ag@ZIF-8 NPs with different silver concentrations

ISSN: 2414-1895 DOI: 10.6919/ICJE.202504_11(4).0037

The content of Ag element in different concentrations of Ag-modified ZIF-8 (Ag@ZIF-8) was investigated by EDS mapping analysis. The results show that the silver element signal is clearly visible in the mapping spectra of Ag@ZIF-8, which proves that the silver element has been successfully doped into the crystal structure of ZIF-8. With the increase of Ag concentration, the content of Ag element gradually increased.

3.3 Biological Properties

In order to evaluate the antimicrobial properties of Ag-modified ZIF-8, we used plate counting method by E. coli and S. aureus studies. The figure 4 compares the antimicrobial effect of ZIF-8 and Ag@ZIF-8 (1% Ag@ZIF-8, 5% Ag@ZIF-8, 10% Ag@ZIF-8) samples doped with different concentrations of silver ions, and the results of the plate cultures show that the antimicrobial performance is significantly enhanced with increasing silver ion concentration for both E. coli and S. aureus. Especially, 10%Ag@ZIF-8 showed an antibacterial rate close to 100%, demonstrating excellent antibacterial effect.

From the analysis of the data of graph antibacterial rate, it can be obtained that silver ion incorporation significantly enhanced the inhibition of E. coli with 68.44%, 72%, and 78.2%, respectively. For Staphylococcus aureus, silver ion admixture similarly enhanced the inhibition rates of 66.3%, 75.2%, and 82.6%, respectively, demonstrating that the antibacterial properties were more moderate in 1% Ag@ZIF-8 samples, but significantly enhanced in 5% Ag@ZIF-8 and 10% Ag@ZIF-8, further demonstrating a positive correlation between the silver ion concentration and antibacterial effect .

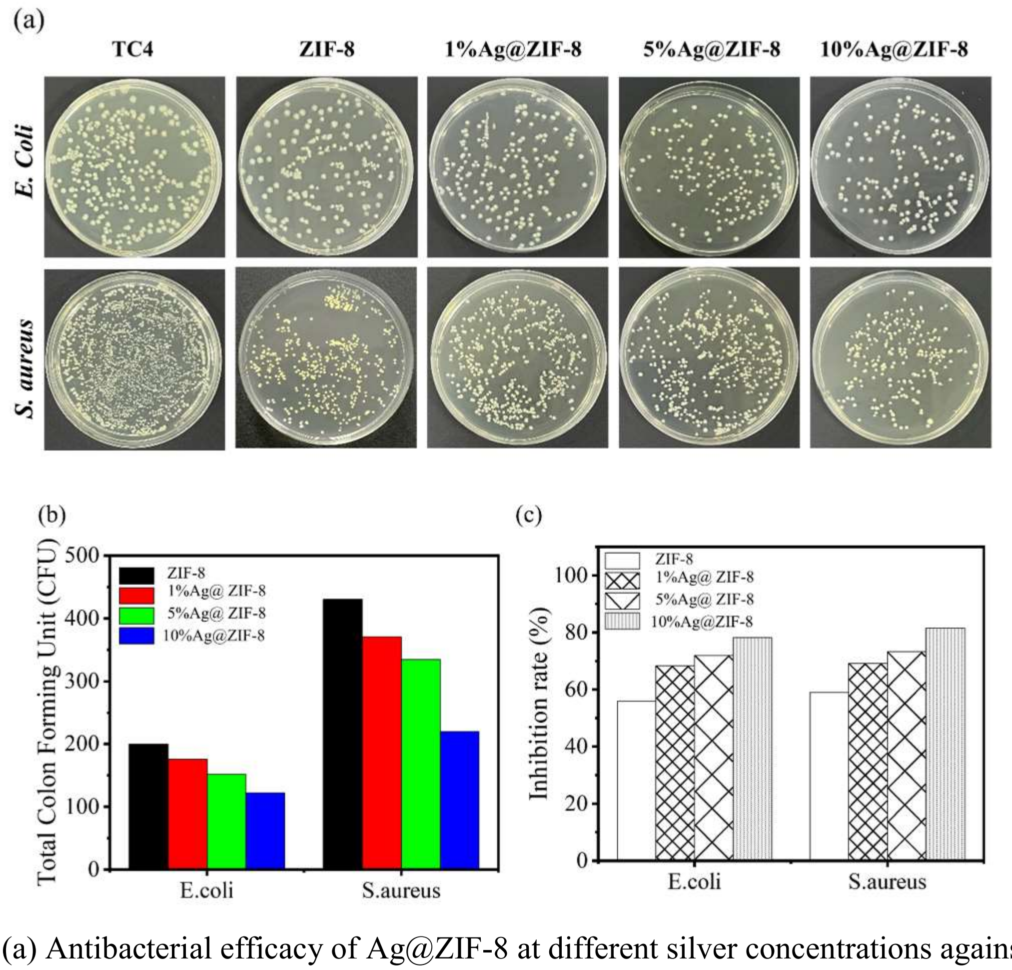

Figure 4. (a) Antibacterial efficacy of Ag@ZIF-8 at different silver concentrations against E. coli and S. aureus (b) CFU of E. coli and S. aureus (c)Antibacterial properties of E. coli and S. Aureus

ISSN: 2414-1895 DOI: 10.6919/ICJE.202504_11(4).0037

The antibacterial mechanism of ZIF-8 is mainly derived from the zinc ions in its framework. Zinc ions have certain antibacterial activity and can inhibit bacterial growth by interfering with bacterial cell membrane function and affecting active enzymes [6]. The silver ions released during the degradation of modified Ag@ZIF-8 in contact with the bacterial cell membrane will activate the relevant enzyme system in the membrane, disturb the ion transport of the cell membrane and change its permeability, thus leading to bacterial death [8]. In addition, at higher concentrations of silver ion doping, silver ions may further inhibit bacterial growth and enhance its antibacterial effect by generating oxidative stress.

4. Conclusion

In this study, the antimicrobial properties were enhanced by modifying gradient silver-modified ZIF-8 nanoparticles (Ag@ZIF-8) on the surface of titanium alloys.ZIF-8 is a porous crystalline material with excellent biocompatibility, and silver nanoparticles have attracted much attention due to their excellent antimicrobial properties. Experimental results showed that the introduction of silver ions significantly enhanced the antimicrobial activity of ZIF-8, especially in 10% Ag@ZIF-8 samples. This study provides a new idea for the enhancement of antimicrobial performance of titanium alloy implants, which has a broad clinical application prospect.

References

[1] J. Xu, J. Zhang, Y. Shi, J. Tang, D. Huang, M. Yan, M.S. Dargusch, Surface Modification of Biomedical Ti and Ti Alloys: A Review on Current Advances, Materials 15 (2022) 1749. https://doi.org/10.3390/ma15051749.

[2] J. Abdi, Synthesis of Ag-doped ZIF-8 photocatalyst with excellent performance for dye degradation and antibacterial activity, Colloids and Surfaces A: Physicochemical and Engineering Aspects 604 (2020) 125330. https://doi.org/10.1016/j.colsurfa.2020.125330.

[3] H.N. Abdelhamid, Zeolitic Imidazolate Frameworks (ZIF-8) for Biomedical Applications: A Review, CMC 28 (2021) 7023–7075. https://doi.org/10.2174/0929867328666210608143703.

[4] M. Li, Y. Wei, B. Ma, Y. Hu, D. Li, X. Cui, Synthesis and Antibacterial Properties of ZIF-8/Ag-Modified Titanium Alloy, J Bionic Eng 19 (2022) 507–515. https://doi.org/10.1007/s42235-021-00135-3.

[5] S. Bao, S. Sun, L. Li, L. Xu, Synthesis and antibacterial activities of Ag-TiO2/ZIF-8, Front. Bioeng. Biotechnol. 11 (2023). https://doi.org/10.3389/fbioe.2023.1221458.

[6] L. Li, J. Zhao, F. Ma, D. He, P. Liu, W. Li, K. Zhang, X. Chen, L. Song, The Mg doping ZIF-8 loaded with Icariin and its antibacterial and osteogenic performances, J Mater Sci: Mater Med 34 (2023) 50. https://doi.org/10.1007/s10856-023-06755-x.

[7] M. Falahaty marvast, M. Gholambargani, M. Ramezanzadeh, B. Ramezanzadeh, Enhancing Self-Healing and Adhesion Bonding Properties: Investigating the Promising Potential of Ce-ZIF8 MOF Hybrid Thin Films as pH-Responsive Nanocoatings, Langmuir 39 (2023) 9579–9594. https://doi.org/10.1021/acs.langmuir.3c01363.

[8] J. Lin, Y. Li, L. Ge, Y. Zhang, S. Yuan, M. Wang, D. Xu, J. Tu, Photothermal enhanced ion release of ZIF-8/Ag/PDA for boosted antimicrobial performance, Inorganic Chemistry Communications 174 (2025) 114001. https://doi.org/10.1016/j.inoche.2025.114001.